Materials Today Communications 29 (2021) 102869

Contents lists available at ScienceDirect

Materials Today Communications

journal homepage: www.elsevier.com/locate/mtcomm

Research on drop-weight impact of continuous carbon fiber reinforced 3D printed honeycomb structure

Hao Dou [a], Wenguang Ye [a], Dinghua Zhang [a], Yunyong Cheng [a,*], Kuidong Huang [a], Fuqiang Yang [a], Stephan Rudykh [b]

[a] School of Mechanical Engineering, Northwestern Polytechnical University, Xi'an, Shaanxi 710072, China
[b] Department of Mechanical Engineering, University of Wisconsin-Madison, WI 53706, USA

ARTICLE INFO

Keywords:
3D printed
Continuous carbon fiber
Honeycomb structure
Drop-weight impact
Failure modes

ABSTRACT

Continuous carbon fiber reinforced 3D printed parts have been widely researched due to their excellent mechanical and thermal properties. This research presents a continuous carbon fiber reinforced 3D printed honeycomb structure, which is manufactured by a modified 3D printer. For comparison, the drop-weight impact test of the honeycomb structure with continuous fiber reinforced and non-reinforced pure matrix of polylactide (PLA) is printed and the results show that the continuous carbon fiber greatly improved the impact resistance of the honeycomb structure. The finite element model is established to simulate the impact process, which is in good agreement with the experimental results. Cone beam computed tomography (CT) is also used to detect the internal damage of honeycomb structure during impact, it is found from the detection images that the main failure modes of the structure are the failure of matrix-fiber interface and the destruction between adjacent printing paths.

1. Introduction

In recent years, additive manufacturing technology has been greatly developed [1]. The advantages such as high design freedom, manufacturing resource saving, fast and complex structure forming contribute additive manufacturing technology to be applied in many fields such as aerospace, automobile, construction and medical treatment [2]. Fused Filament Fabrication (FFF) 3D printing technology is an extremely widely used additive manufacturing molding technology with relatively simple process which has great development and application potential, since FFF can manufacture functional parts with complex geometric shapes, which can be improved as an alternative method for the traditional molding process of fiber reinforced composite either [3–5]. The common components of fiber-reinforced 3D printed composites are mainly divided into two parts: continuous fibers represented by carbon fiber, glass fiber and Kevlar fiber, and matrix materials represented by PLA, Acrylonitrile Butadiene Styrene (ABS) and polyether ether ketone (PEEK) [6].

Continuous carbon fiber reinforced thermoplastic composites are becoming more and more important in industrial applications as their excellent mechanical properties, easy machinability and recoverability of light weight structures [7]. In the past several years, the basic mechanical properties of continuous carbon fiber reinforced 3D printed parts, such as tensile, compression and bending, have been widely studied. As the reinforcement phase, continuous carbon fiber has greatly improved the mechanical properties of the structure. In addition, in order to further understand the factors affecting the strength of continuous carbon fiber reinforced 3D printed composites, relevant researches on the printing process parameters [8], fiber modification [9–11] and fiber-matrix [12,13] impregnation have also been carried out.

Low-density, porous solid structures widely exist in nature and have excellent physical and mechanical properties [14,15]. The low-density feature allows the design of lightweight and rigid structural parts, such as sandwich structures [16] and large portable components, researchers have conducted detailed studies on their structure, mechanics, thermals, and other properties [17–19]. The solid honeycomb structures are composed of solid pillars and plate structures that form the boundary and surface of the cell body. The shape has a complete hexagonal structure and disordered sponge and bone structures [20]. The characteristics of the honeycomb structure mainly depend on the thickness of the cell body wall and the arrangement method, so it is necessary to

* Corresponding author.
E-mail address: chengyunyong@nwpu.edu.cn (Y. Cheng).

https://doi.org/10.1016/j.mtcomm.2021.102869
Received 5 July 2021; Received in revised form 24 September 2021; Accepted 26 September 2021
Available online 2 November 2021

carry out research on the control cell body shape and arrangement, and establish the quantitative relationship between the relative density with the thickness and length of the cell body, according to which, many scholars have conducted research on the mechanical and thermal properties of aluminum [21,22], paper [23] and resin hexagonal honeycomb structures.

Previous related researches mainly focused on the tensile, compression and bending properties of continuous fiber reinforced composites, and there is relatively few research on their impact properties [24,25]. Different solutions available in the literature to solve this problem have been reviewed, the impact resistance of different configurations of continuous fiber reinforced sandwich structures is related to the thickness and height of the core [26], and the impact resistance of the composite structure formed by additive manufacturing is mainly affected by the pattern, arrangement direction of the fiber [27] and the direction of the layer stacking [25]. Through experimental test results, it is found that under drop-weight impact load, the impact resistance and energy absorption capacity of carbon fiber reinforced composites are significantly improved [28]. In addition, non-destructive testing is used to evaluate the defects of the composites during the molding process and the damage after impact [29].

This paper proposes a lightweight continuous carbon fiber reinforced 3D printed honeycomb structure, which is printed by a modified FFF 3D printer. The whole structure and printing path of the test piece is designed to ensure fiber continuity and quality reliability. Research on its drop-weight impact performance mainly includes impact resistance and energy absorption capacity. Comparison test results found that the continuous carbon fiber reinforced 3D printed honeycomb structure has a significant improvement in impact performance. In this paper, the finite element simulation model is also compared and verified with the test results, and the two are more consistent. In this paper, a finite element (FE) simulation model is also established, and good agreement is achieved among FE simulation results and experimental tests.

2. Preparation of specimens

2.1. Materials: Carbon fiber and PLA

In the preparation process of the specimens, 1 K continuous carbon fiber (HTA 40, Toho Tenax Co., Ltd, Japan) is selected as the reinforcing phase and PLA (FlashForge, Hangzhou, Zhejiang, China) is used as the matrix. Continuous carbon fiber is a kind of strategic material with excellent mechanical properties, including good high temperature resistance, high wear resistance, good electrical and thermal conductivity, and corrosion resistance, the carbon content of which is generally above 90%. As the result, continuous carbon fiber has better processability and engineering application value, since it has significant anisotropy, high strength along the fiber direction, small specific gravity and high specific strength [30]. The general continuous carbon fiber bundle used in the current researches is composed of fiber filaments with a diameter of 5–10 μm, and the number of fiber filaments in the fiber bundle ranges from 1 K to 5 K. It can be seen from Fig. 1(a), as a kind of Tenax series carbon fiber, HTA 40 is suitable for various processing techniques, which has a good impregnation rate and good processability. The surface treatment of this kind of fiber improves the adhesion strength between the carbon fiber and the matrix, which can protect the fiber.

PLA is a new type of biodegradable material with good thermal stability and ductility, and can be better adapted to the FFF manufacturing. Moreover, PLA is widely used in a wide range of application since it has excellent mechanical and physical properties, and its high specific stiffness and specific strength make it suitable for the manufacture of lightweight structures [31–33]. It should be noted that PLA has a certain hygroscopicity, too much water vapor inhalation will reduce the mechanical strength, so it is necessary to dry the PLA filament before the preparation of the experimental specimens. As shown in Fig. 1 (b), the weight of PLA coil used in this paper is 1 kg, and the diameter of PLA filament is 1.75 mm ± 0.02 mm. The basic mechanical parameters of carbon fiber and PLA are shown in Table 1:

2.2. Preparation of specimens

The 3D printer presented in this paper is a desktop Reprap-Kossel 3D printer as the prototype, combining with the characteristics of the melt deposition molding, the nozzle is properly modified, as shown in Fig. 2 (a), so that the plasticized thermoplastic and continuous carbon fiber are extruded from the nozzle and adhered to the printing platform under the internal pressure of the deposition chamber.

The basic process parameters of specimen printing are shown in Table 2.

The honeycomb structure adopted in this paper is composed of regular hexagon, and the overall configuration of the specimens is shown in Fig. 3(a). Due to the process limitation of continuous fiber reinforced 3D printing, the thickness of inclined wall and horizontal wall

Table 1
Basic mechanical parameters of continuous carbon fiber and PLA [19].

	Tensile strength	Tensile modulus	Elongation at break	Density
HTA 40	4100 MPa	240 GPa	1.7%	1.78 g cm^{-3}
PLA filament	62.63 MPa	3.2 GPa	4.43%	1.24 g cm^{-3}

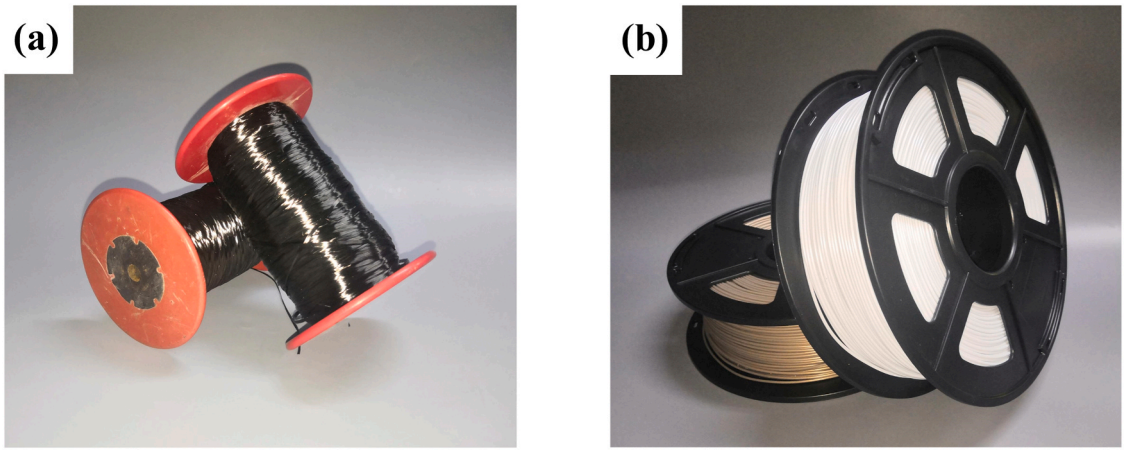

Fig. 1. Continuous carbon fiber and PLA filament.

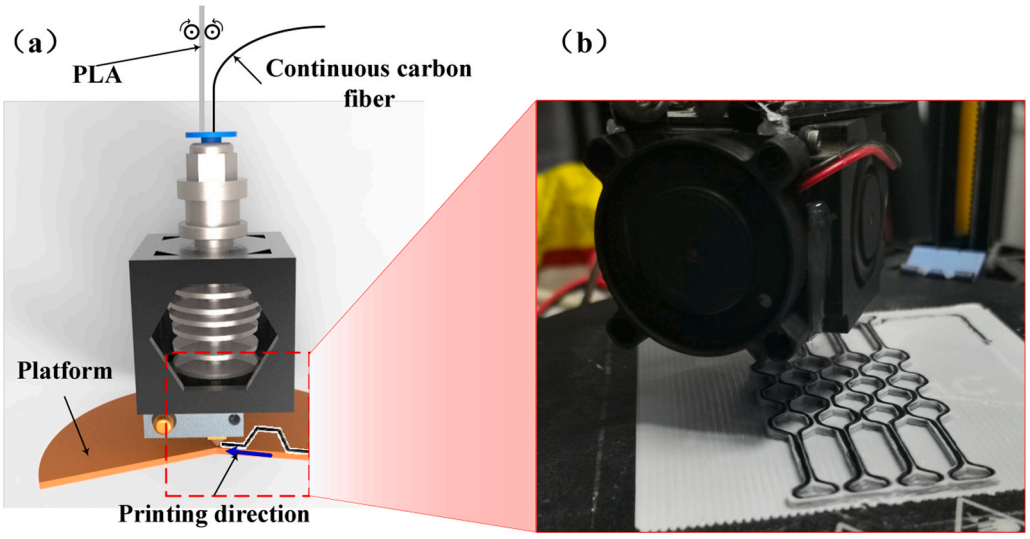

Fig. 2. Continuous carbon fiber reinforced composite printing scheme: (a) printing head imaging, (b) printing process.

Table 2
Printing process parameters.

Printing height (H)	Extrusion width (W)	Nozzle temperature (T)	Extrusion speed (V)	Platform temperature (T_p)	Filling density
0.3 mm	1.5 mm	210 ℃	100 mm min^{-1}	50 ℃	100%

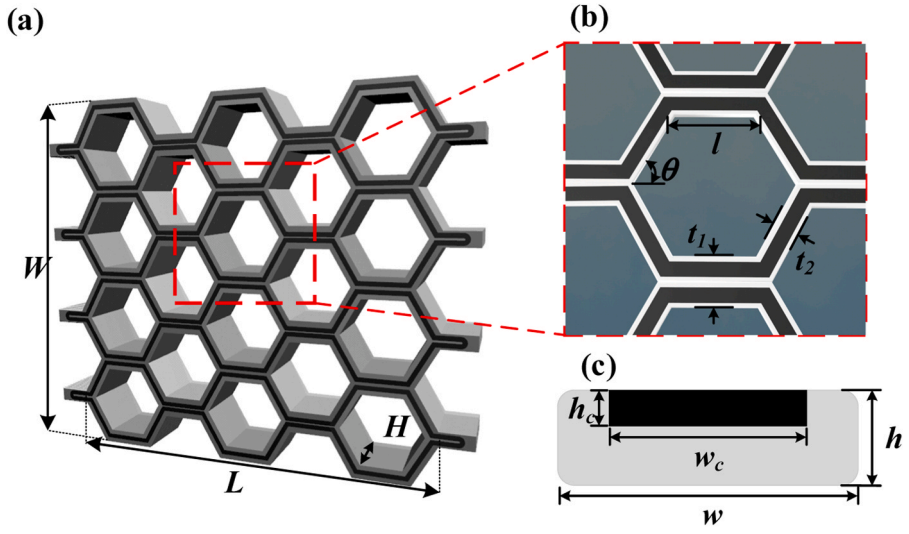

Fig. 3. The parametric model of the specimens: (a) honeycomb structure, (b) the parametric model of the honeycomb unit, (c) the print path cross section.

in honeycomb is different, which is distinguished by t_1 and t_2 in the figure. For continuous carbon fiber reinforced honeycomb structure, the cross-section of single-layer is shown in Fig. 3(c).

The mechanical properties of continuous carbon fiber reinforced 3D printed composites are affected by a series of process parameters, such as layer height, extrusion width, printing temperature and printing speed. The printing layer height and extrusion width will affect the relative carbon content (including fiber volume fraction and fiber mass fraction) of the structure, and then indirectly affect the mechanical properties of the composites [8]. The relative density of the honeycomb is the main factor that impacts the mechanical properties when the cell topology is unchanged and the printing extrusion width and layer height are fixed, which is defined as the ratio of the density of the honeycomb structure to that of the solid from which the cell walls are made. Under the condition of neglecting the small corner area, the rough calculation method of relative density ρ_r is as follows [19]:

$$\rho_r = \frac{\rho}{\rho_s} = \frac{t_1 + 2t_2}{2l\sin\theta + l\sin 2\theta} \times 100\% \tag{1}$$

Where, ρ and ρ_s denote the density of the honeycomb structure and the density of the solid from which the cell walls are made defined above respectively. The unit structures used in this paper are all regular hexagons, $\theta = 60°$, substituting it into formula (1), the following result is obtained:

$$\rho_r = \frac{2}{3\sqrt{3}} \frac{t_1 + 2t_2}{l} \times 100\% \tag{2}$$

According to the section parameters in Fig. 3(c), the relative carbon

fiber mass fraction and fiber volume fraction can be roughly calculated as:

$$\omega_c = \frac{M_c}{M_a} = \frac{w_c h_c \rho_c}{(wh - w_c h_c)\rho_m + w_c h_c \rho_c} \times 100\% \quad (3)$$

Where M_c and M_a are the unit mass of carbon fiber and the structure, respectively, ρ_c is the density of carbon fiber and ρ_m is the density of matrix.

$$V_f = \frac{V_c}{V_a} = \frac{w_c h_c}{wh} \times 100\% \quad (4)$$

Where V_c and V_a represent the volume of carbon fiber and the total volume of material respectively.

By substituting the data into Eqs. (2–4), the relative density and carbon fiber mass fraction and fiber volume fraction of the continuous carbon fiber reinforced 3D printed honeycomb structure are 39.53%, 21.47% and 16% respectively.

In the process of 3D printing, as shown in Fig. 4(a), the extruded material is gradually cooled on the platform, while the placement of the fiber is dragged by the tensile force of the formed part. Therefore, there is a certain resistance in the pull-out of the carbon fiber, which leads to the fiber clinging to the side of the nozzle opposite to the printing direction [34]. Large area of "fiber free area" and "matrix-fiber separation area" will appear in the place with large molding path angle, as shown in Fig. 4(b-c), which will affect the mechanical properties of the structures. Therefore, by optimizing the printing parameters and further improving the parametric model of structural design, the auxiliary structure is designed at both ends of the specimen, as shown in Fig. 4(d). After printing, the mechanical post-processing is carried out to process the designed specimen. And in the drop-weight impact test, the auxiliary structure can be used for clamping so that the mechanical properties of the specimens are retained to the maximum.

3. Experiment and FE simulation of drop-weight impact

3.1. Equipment

In order to evaluate the drop-weight impact performance of continuous carbon fiber reinforced 3D printed honeycomb, as shown in Fig. 5, a drop-weight impact system (INSTRON-CEAST 9340, Boston USA) was used. CEAST 9340 is a floor type system, which is widely used in a variety of impact tests. The energy transfer range is 0.30–405 J, the impact velocity range is 0.77–4.65 m s^{-1}, the drop height is 0.03–1.10 m, and the drop weight is 1.00–37.5 kg.

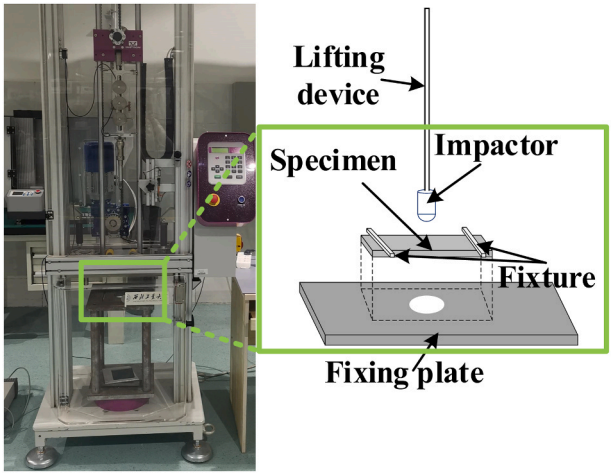

Fig. 5. Drop-weight impact system.

As shown in Fig. 5, the impactor is made of steel with ball head of 20 mm in diameter, which can be regarded as rigid body, the sample is fixed on the plate by two clamping fixtures, and a circular hole with a diameter of 75 mm is set in the center of the fixing plate. When installing the experimental pieces, the center of the hole and the geometric center of the specimen coincide with the impact point of impactor so as to ensure the symmetry of the constraint, and the impactor can pass through the geometric center of the sample along the vertical direction. The weight of impactor is 3.73 kg in this research, the specimen can be impacted with different energy by falling freely along the guide tube in the impact system at different heights. Since the impactor can be regarded as a rigid body, the displacement of the impactor is the deformation at the geometric center of the specimen.

The energy absorbed by the specimen during impact is calculated by the following formula:

$$E = m_I g h_I \quad (5)$$

Where m_I is the mass of the impactor, g is the acceleration of gravity, and

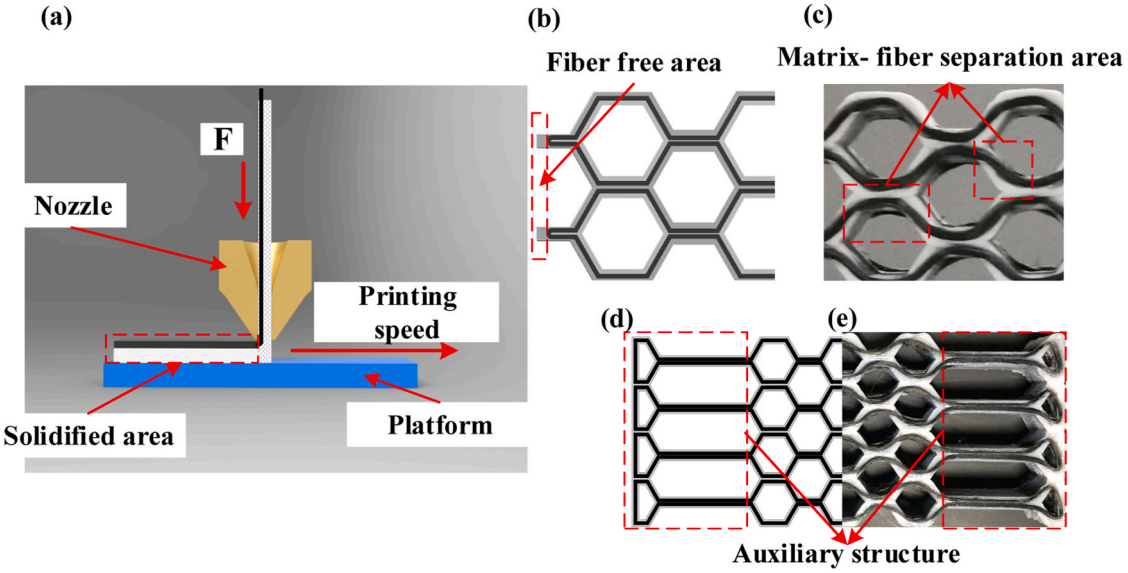

Fig. 4. The optimization design of the honeycomb: (a) fiber traction and placement, (b) fiber blank defect, (c) matrix fiber separation defect, (d) model sketch of structure optimization, (E) 3D printed optimized specimen.

h_I is the falling height of the impactor.

3.2. Finite element simulation modeling

In this paper, the finite element simulation model of continuous carbon fiber reinforced honeycomb structure is established, and the commercial finite element software ABAQUS is used to simulate the impact test and verify the experimental results. The 3D model of honeycomb is shown in Fig. 3(a), and its finite element model is established by combining its printing path, material properties and structural geometric parameters of matrix and continuous carbon fiber are shown in Table 1 and Fig. 3. While establishing the FE model, PLA is defined as isotropy, and its elastic and plastic parameters are calculated according to the previous experimental results. In order to simplify the simulation, continuous carbon fiber is considered as isotropy either [18], it is important to note that this kind of simplification only presents in the FE model, and there is no correlation with the subsequent experimental results. The impactor is a rigid body and its contact with the honeycomb is defined as penalty. The established FE model is shown in Fig. 6:

3.3. Analysis

In order to better present the impact resistance of continuous carbon fiber reinforced honeycomb, the experimental results of reinforced honeycomb and unreinforced honeycomb are compared in this section. In the comparative experiment, the relative density of honeycomb structure is both 39.53%.

The first impact energy is 2 J when testing the honeycomb structure of pure matrix, and obvious cracks appear after the deformation of the specimen, resulting in complete failure. After adjusting the impact energy for several times, when the initial energy is reduced to 1.5 J, no conspicuous damage emerges on the surface of the structure after the impact, as shown in Fig. 7(a-b), and Fig. 7(c) shows the change of impact force and energy with time.

According to the previous research results of the tensile strength test [8], the mechanical property of continuous carbon fiber reinforced honeycomb structure is estimated to be 4–8 times higher than that of pure PLA, combined with the above experimental results, the energy selected for the first impact test is 10 J, and the experimental results are shown in Fig. 8(a). It can be seen that specimen fractured along the direction perpendicular to the carbon fiber and completely failed. When the energy is reduced to 5 J, the specimen appears microcracks along the direction of carbon fiber reinforcement, i.e. printing direction, and no carbon fiber fracture is revealed, as shown in Fig. 8(b), Fig. 8(c) shows the change of impact force and energy with time when the impact energy is 5 J.

This paper elaborates the impact resistance when there is no obvious damage on the surface of the pure PLA honeycomb, and the continuous carbon fiber reinforced honeycomb is damaged in the matrix and the fiber is in good condition. As well as the specific energy absorption of the two structures is calculated according to the experimental results to better evaluate the energy absorption capacity of the structure. The specific energy absorption E_S can be calculated as:

$$E_S = \frac{E}{m_s} \tag{6}$$

Where E is the energy absorbed by the honeycomb and m_s is the mass of the structure.

The results under pre-defined failure conditions are shown in Fig. 9, the calculated impact forces of two different materials are 512 N and 1353 N, and the specific energy absorption is 173 J kg^{-1} and 537 J kg^{-1} respectively.

Fig. 10 presents the FE analysis and experimental results, and compares the force and energy absorption of continuous carbon fiber reinforced honeycomb structure from the penetrator under impact. According to the trend of the curve, the experiment and simulation of that two analysis objects show good consistency, which confirms the applicability of the FE model established in this section.

3.4. Damage assessment

According to the experimental results, the bearing capacity of continuous fiber reinforced honeycomb under drop-weight impact has a certain gap with the expected value and the FE simulation results. In order to better evaluate the impact resistance of the structure, the industrial cone beam CT nondestructive testing is used to detect the internal damage of honeycomb caused by impact, the detection parameters of industrial cone beam CT are as follows [35]: DSD(Distance between source and detector)= 1222 mm, DSO(Distance between source and origin)= 872 mm, scanning angle and the number of circular projections are 360° and 720 respectively, the diameter of the source is 0.4 mm, voltage and current of the source are 100 kV and 1.2 mA respectively.

The detection image is shown in Fig. 11, obvious internal stratification phenomenon appears in the structure after impact, as shown in Fig. 11(b). According to the number of CT scanning image layers, the layered part occurs in the upper of the structure, that is, the impact will change the interlaminar state of the specimen, which will cause separation between the printing layers and the failure of fiber-matrix interface. Fig. 11 (c) shows the failure of the matrix while the crack is almost

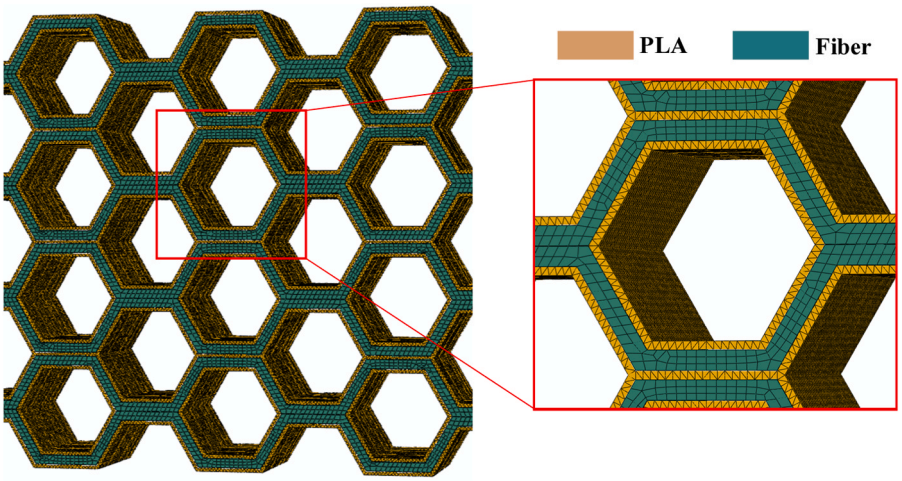

Fig. 6. FE model.

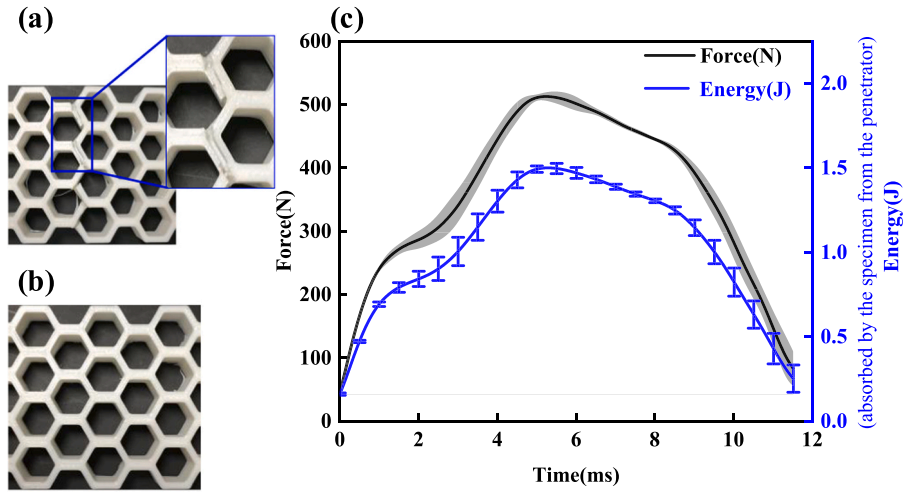

Fig. 7. The impact test results of pure PLA honeycomb: (a) impact energy is 2 J, (b) impact energy is 1.5 J, (c) energy (absorbed by the specimen from the penetrator) -time curve and force-time curve (1.5 J).

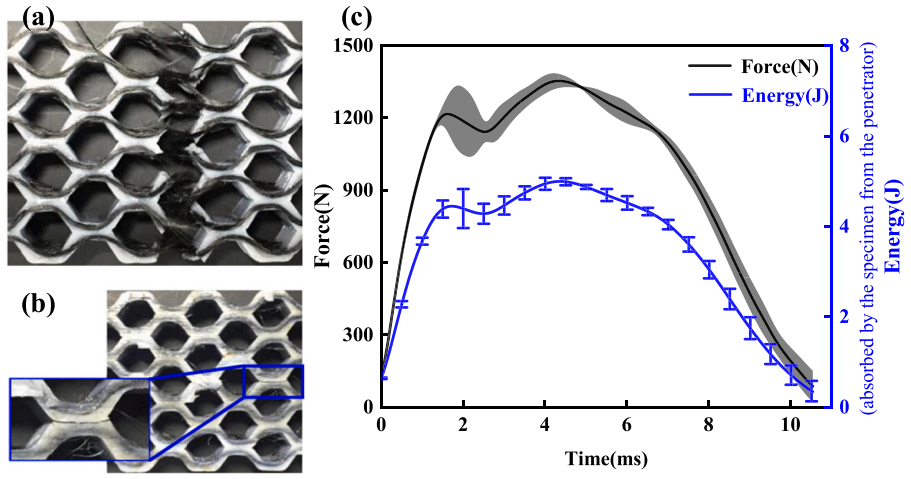

Fig. 8. The impact test results of continuous carbon fiber reinforced honeycomb: (a) impact energy is 10 J, (b) impact energy is 5 J, (c) energy (absorbed by the specimen from the penetrator)-time curve and force-time curve (5 J).

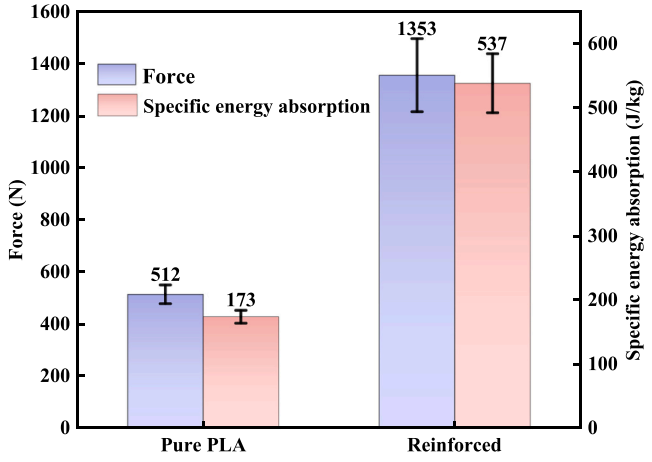

Fig. 9. Comparison of impact force and specific energy absorption of honeycomb with different materials.

parallel to the fiber direction, and spreads in all slices, which causes the crack to penetrate the whole part. It can be concluded that the bonding strength between adjacent printing paths is an important factor restricting the mechanical properties of the structure, and it is also a manifestation of the poor impregnation of the matrix-fiber.

4. conclusion

The continuous carbon fiber reinforced 3D printed honeycomb is presented in this research, printing process of the honeycomb is designed and drop-weight impact are carried out. A new Finite Element analysis method of the complex structure is proposed, as well as the cone beam CT is used for nondestructive testing to analyze the failure modes of the specimen. The main conclusions are as follows:

1. Combined with the printing path of continuous carbon fiber reinforced honeycomb, the Finite Element simulation model of the structure is established, and the simulation results are in good agreement with the experimental results.
2. The failure modes of continuous carbon fiber reinforced honeycomb specimens under drop-weight impact can be divided into fiber fracture perpendicular to the direction of carbon fiber, matrix crack along the printing direction, and collapse of the interface with

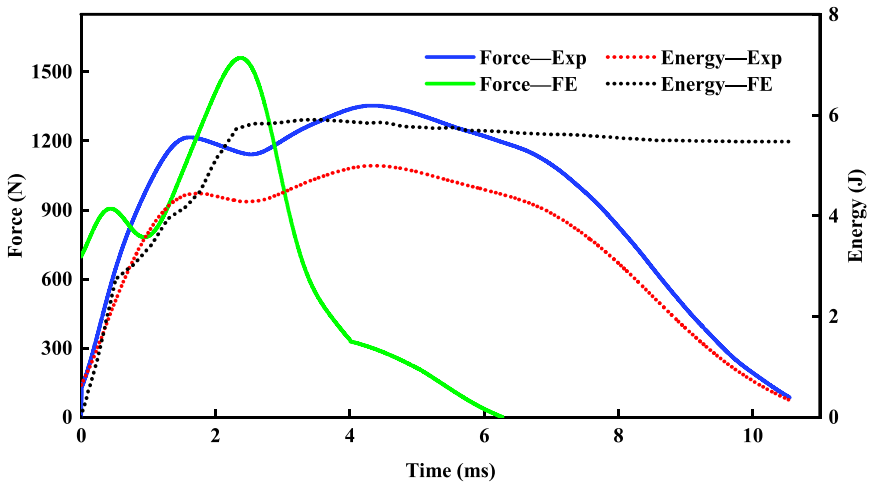

Fig. 10. Comparison of FE analysis and experimental results.

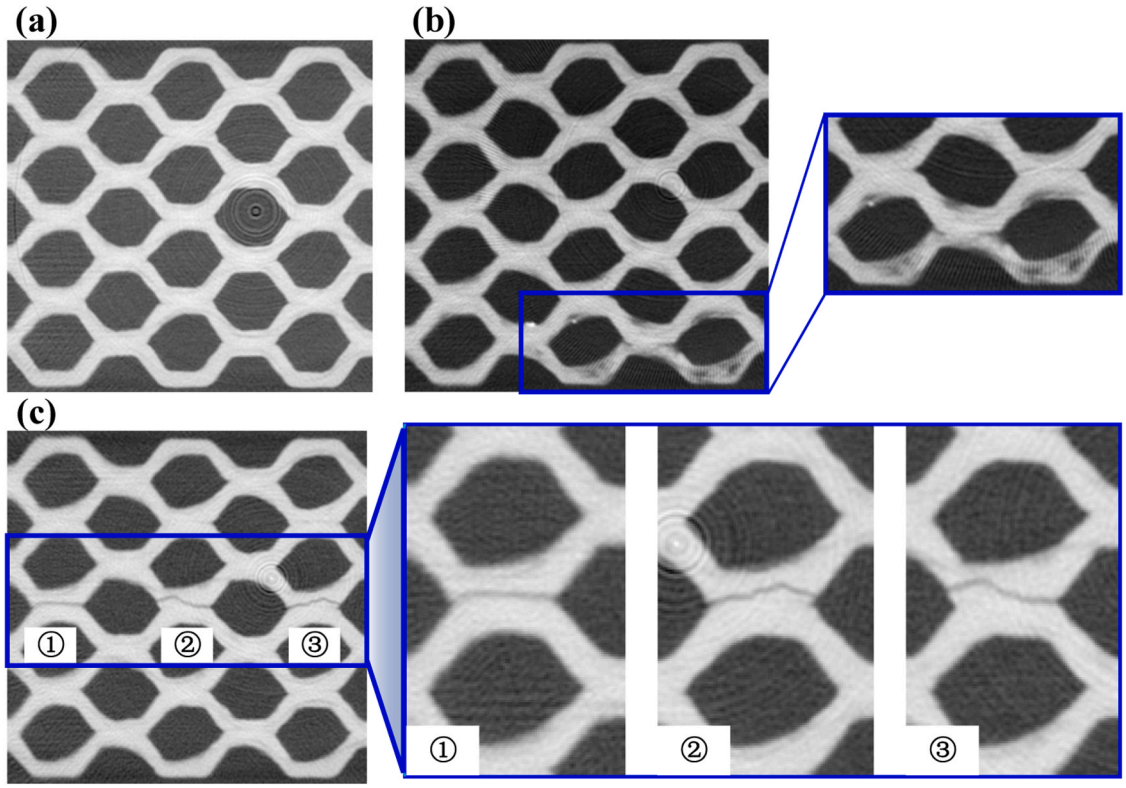

Fig. 11. The industrial cone beam CT detection results of continuous fiber reinforced honeycomb: (a) original specimen, (b) delamination caused by impact, (c) matrix fracture.

impactor. With the increase of impact energy, the bearing mode changes from matrix deformation to longitudinal tensile of carbon fiber.

3. According to the experimental results, the impact force and absorbed energy of continuous carbon fiber reinforced honeycomb is about 3–4 times that of pure PLA. In particular, it should be noted that the matrix crack is considered as failure in the tests, instead of the breaking of carbon fiber, while the impact resistance of the structure is higher under these circumstances.
4. From the scanning results of cone beam CT, it is easy to know that the main failure modes of the specimen are interlaminar splitting and matrix-fiber interface failure. The impregnation of the matrix-fiber in continuous carbon fiber reinforced 3D printed honeycomb is an important factor affecting its mechanical properties.

Furthermore, in order to establish a refined FE model to better restore the experimental process, the stress perpendicular to the fiber direction, normal and shear stress between the CF and PLA layers, interfacial strength between fiber and matrix are planned to investigated.

CRediT authorship contribution statement

Hao Dou: Conceptualization, Data curation, Investigation, Writing - Original Draft, Writing - Review & Editing. **Wenguang Ye:** Data

curation, Investigation. **Dinghua Zhang:** Conceptualization, Writing - Review & Editing. **Yunyong Cheng:** Conceptualization, Writing - Review & Editing. **Kuidong Huang:** Writing - Review & Editing. **Fuqiang Yang:** Data curation, Investigation, Writing - Review & Editing. **Stephan Rudykh:** Writing - Review & Editing. All authors have read and agreed to the published version of the manuscript.

Declaration of Competing Interest

The authors declare that they have no known competing financial interests or personal relationships that could have appeared to influence the work reported in this paper.

Acknowledgments

This research was sponsored by Innovation Foundation for Doctor Dissertation of Northwestern Polytechnical University (CX2021013).

References

[1] X. Wang, M. Jiang, Z. Zhou, J. Gou, D. Hui, 3D printing of polymer matrix composites: a review and prospective, Compos. Part B Eng. 110 (2017) 442–458, https://doi.org/10.1016/j.compositesb.2016.11.034.
[2] T.D. Ngo, A. Kashani, G. Imbalzano, K.T.Q. Nguyen, D. Hui, Additive manufacturing (3D printing): a review of materials, methods, applications and challenges, Compos. Part B Eng. 143 (2018) 172–196, https://doi.org/10.1016/j.compositesb.2018.02.012.
[3] M. Heidari-Rarani, M. Rafiee-Afarani, A.M. Zahedi, Mechanical characterization of FFF 3D printing of continuous carbon fiber reinforced PLA composites, Compos. Part B Eng. 175 (2019), https://doi.org/10.1016/j.compositesb.2019.107147.
[4] N.A.S. Mohd Pu'ad, R.H. Abdul Haq, H. Mohd Noh, H.Z. Abdullah, M.I. Idris, T. C. Lee, Review on the fabrication of fused deposition modelling (FFF) composite filament for biomedical applications, Mater. Today Proc. (2019) 228–232, https://doi.org/10.1016/j.matpr.2020.05.535.
[5] H. Zhao, X. Liu, W. Zhao, G. Wang, B. Liu, An overview of research on FFF 3D printing process of continuous fiber reinforced composites, J. Phys. Conf. Ser. 1213 (2019), https://doi.org/10.1088/1742-6596/1213/5/052037.
[6] S.H.R. Sanei, D. Popescu, 3D-printed carbon fiber reinforced polymer composites: a systematic review, J. Compos. Sci. 4 (2020) 98, https://doi.org/10.3390/jcs4030098.
[7] H. Liu, J. Liu, Y. Ding, J. Zheng, X. Kong, J. Zhou, L. Harper, B.R.K. Blackman, A. J. Kinloch, J.P. Dear, The behaviour of thermoplastic and thermoset carbon fibre composites subjected to low-velocity and high-velocity impact, J. Mater. Sci. 55 (2020) 15741–15768, https://doi.org/10.1007/s10853-020-05133-0.
[8] H. Dou, Y. Cheng, W. Ye, D. Zhang, J. Li, Z. Miao, S. Rudykh, Effect of process parameters on tensile mechanical properties of 3d printing continuous carbon fiber-reinforced PLA composites, Materials (2020) 3850, https://doi.org/10.3390/ma13173850.
[9] J. Qiao, Y. Li, L. Li, Ultrasound-assisted 3D printing of continuous fiber-reinforced thermoplastic (FRTP) composites, Addit. Manuf. 30 (2019), https://doi.org/10.1016/j.addma.2019.100926.
[10] A. Bashiri Rezaie, M. Liebscher, M. Ranjbarian, F. Simon, C. Zimmerer, A. Drechsler, R. Frenzel, A. Synytska, V. Mechtcherine, Enhancing the interfacial bonding between PE fibers and cementitious matrices through polydopamine surface modification, Compos. Part B Eng. 217 (2021), https://doi.org/10.1016/j.compositesb.2021.108817.
[11] J. Zhuoda, Effects of plasma treatment of carbon fibers on interfacial properties of BMI resin composites, Surf. Interface Anal. 51 (2019) 458–464, https://doi.org/10.1002/sia.6600.
[12] D.J. Kwon, N.S.R. Kim, Y.J. Jang, H.H. Choi, K. Kim, G.H. Kim, J. Kong, S.Y. Nam, Impacts of thermoplastics content on mechanical properties of continuous fiber-reinforced thermoplastic composites, Compos. Part B Eng. 216 (2021) 1–8, https://doi.org/10.1016/j.compositesb.2021.108859.
[13] F. Wang, G. Wang, F. Ning, Z. Zhang, Fiber–matrix impregnation behavior during additive manufacturing of continuous carbon fiber reinforced polylactic acid composites, Addit. Manuf. 37 (2021), 101661, https://doi.org/10.1016/j.addma.2020.101661.
[14] J. Xiong, L. Ma, A. Stocchi, J. Yang, L. Wu, S. Pan, Bending response of carbon fiber composite sandwich beams with three dimensional honeycomb cores, Compos. Struct. 108 (2014) 234–242, https://doi.org/10.1016/j.compstruct.2013.09.035.
[15] S.R.G. Bates, I.R. Farrow, R.S. Trask, Compressive behaviour of 3D printed thermoplastic polyurethane honeycombs with graded densities, Mater. Des. 162 (2019) 130–142, https://doi.org/10.1016/j.matdes.2018.11.019.
[16] J. Xiong, M. Zhang, A. Stocchi, H. Hu, L. Ma, L. Wu, Z. Zhang, Mechanical behaviors of carbon fiber composite sandwich columns with three dimensional honeycomb cores under in-plane compression, Compos. Part B Eng. 60 (2014) 350–358, https://doi.org/10.1016/j.compositesb.2013.12.049.
[17] Y. Chen, T. Li, Z. Jia, F. Scarpa, C.W. Yao, L. Wang, 3D printed hierarchical honeycombs with shape integrity under large compressive deformations, Mater. Des. 137 (2018) 226–234, https://doi.org/10.1016/j.matdes.2017.10.028.
[18] C. Quan, B. Han, Z. Hou, Q. Zhang, X. Tian, T.J. Lu, 3D printed continuous fiber reinforced composite auxetic honeycomb structures, Compos. Part B Eng. 187 (2020), 107858, https://doi.org/10.1016/j.compositesb.2020.107858.
[19] Y. Cheng, J. Li, X. Qian, S. Rudykh, 3D printed recoverable honeycomb composites reinforced by continuous carbon fibers, Compos. Struct. 268 (2021), https://doi.org/10.1016/j.compstruct.2021.113974.
[20] B.G. Compton, J.A. Lewis, 3D-printing of lightweight cellular composites, Adv. Mater. 26 (2014) 5930–5935, https://doi.org/10.1002/adma.201401804.
[21] S. Shi, Z. Sun, X. Hu, H. Chen, Flexural strength and energy absorption of carbon-fiber-aluminum-honeycomb composite sandwich reinforced by aluminum grid, Thin-Walled Struct. 84 (2014) 416–422, https://doi.org/10.1016/j.tws.2014.07.015.
[22] S.S. Shi, Z. Sun, X.Z. Hu, H.R. Chen, Carbon-fiber and aluminum-honeycomb sandwich composites with and without Kevlar-fiber interfacial toughening, Compos. Part A Appl. Sci. Manuf. 67 (2014) 102–110, https://doi.org/10.1016/j.compositesa.2014.08.017.
[23] D. Wang, N. Liang, Y. Guo, Finite element analysis on the out-of-plane compression for paper honeycomb, J. Strain Anal. Eng. Des. 54 (2019) 36–43, https://doi.org/10.1177/0309324718812527.
[24] M. Vaško, M. Sága, J. Majko, A. Vaško, M. Handrik, Impact toughness of frtp composites produced by 3D printing, Materials (2020) 1–23, https://doi.org/10.3390/ma13245654.
[25] D.R. Hetrick, S.H.R. Sanei, O. Ashour, C.E. Bakis, Charpy impact energy absorption of 3D printed continuous Kevlar reinforced composites, J. Compos. Mater. 55 (2021) 1705–1713, https://doi.org/10.1177/0021998320985596.
[26] S. Zangana, J. Epaarachchi, W. Ferdous, J. Leng, P. Schubel, Behaviour of continuous fibre composite sandwich core under low-velocity impact, Thin-Walled Struct. 158 (2021), https://doi.org/10.1016/j.tws.2020.107157.
[27] S.M.F. Kabir, K. Mathur, A.F.M. Seyam, Impact resistance and failure mechanism of 3D printed continuous fiber-reinforced cellular composites, J. Text. Inst. 112 (2021) 752–766, https://doi.org/10.1080/00405000.2020.1778223.
[28] Y. Delporte, H. Ghasemnejad, Manufacturing of 3D printed laminated carbon fibre reinforced nylon composites: impact mechanics, J. Compos. Mater. 11 (2021) 1–11, https://doi.org/10.4236/ojcm.2021.111001.
[29] M.A. Caminero, I. García-Moreno, G.P. Rodríguez, J.M. Chacón, Internal damage evaluation of composite structures using phased array ultrasonic technique: impact damage assessment in CFRP and 3D printed reinforced composites, Compos. Part B Eng. 165 (2019) 131–142, https://doi.org/10.1016/j.compositesb.2018.11.091.
[30] N. van de Werken, H. Tekinalp, P. Khanbolouki, S. Ozcan, A. Williams, M. Tehrani, Additively manufactured carbon fiber-reinforced composites: state of the art and perspective, Addit. Manuf. 268 (2021), https://doi.org/10.1016/j.addma.2019.100962.
[31] R.T.L. Ferreira, I.C. Amatte, T.A. Dutra, D. Bürger, Experimental characterization and micrography of 3D printed PLA and PLA reinforced with short carbon fibers, Compos. Part B Eng. 124 (2017) 88–100, https://doi.org/10.1016/j.compositesb.2017.05.013.
[32] S. Farah, D.G. Anderson, R. Langer, Physical and mechanical properties of PLA, and their functions in widespread applications — a comprehensive review, Adv. Drug Deliv. Rev. 107 (2016) 367–392, https://doi.org/10.1016/j.addr.2016.06.012.
[33] X. Tian, T. Liu, C. Yang, Q. Wang, D. Li, Interface and performance of 3D printed continuous carbon fiber reinforced PLA composites, Compos. Part A Appl. Sci. Manuf. 88 (2016) 198–205, https://doi.org/10.1016/j.compositesa.2016.05.032.
[34] Z. Hou, X. Tian, Z. Zheng, J. Zhang, L. Zhe, D. Li, A.V. Malakhov, A.N. Polilov, A constitutive model for 3D printed continuous fiber reinforced composite structures with variable fiber content, Compos. Part B Eng. 189 (2020), 107893, https://doi.org/10.1016/j.compositesb.2020.107893.
[35] F. Yang, D. Zhang, H. Zhang, K. Huang, Cupping artifacts correction for polychromatic X-ray cone-beam computed tomography based on projection compensation and hardening behavior, Biomed. Signal Process. Control. 57 (2020), 101823, https://doi.org/10.1016/j.bspc.2019.101823.